Development 136, 541-549 (2009) doi:10.1242/dev.029959

Two ParaHox genes, *SpLox* and *SpCdx*, interact to partition the posterior endoderm in the formation of a functional gut

Alison G. Cole[1,*], Francesca Rizzo[1,*], Pedro Martinez[2], Montserrat Fernandez-Serra[1] and Maria I. Arnone[1,†]

We report the characterization of the ortholog of the *Xenopus XlHbox8* ParaHox gene from the sea urchin *Strongylocentrotus purpuratus, SpLox*. It is expressed during embryogenesis, first appearing at late gastrulation in the posterior-most region of the endodermal tube, becoming progressively restricted to the constriction between the mid- and hindgut. The physiological effects of the absence of the activity of this gene have been analyzed through knockdown experiments using gene-specific morpholino antisense oligonucleotides. We show that blocking the translation of the *SpLox* mRNA reduces the capacity of the digestive tract to process food, as well as eliminating the morphological constriction normally present between the mid- and hindgut. Genetic interactions of the *SpLox* gene are revealed by the analysis of the expression of a set of genes involved in endoderm specification. Two such interactions have been analyzed in more detail: one involving the midgut marker gene *Endo16*, and another involving the other endodermally expressed ParaHox gene, *SpCdx*. We find that *SpLox* is able to bind *Endo16* cis-regulatory DNA, suggesting direct repression of Endo16 expression in presumptive hindgut territories. More significantly, we provide the first evidence of interaction between ParaHox genes in establishing hindgut identity, and present a model of gene regulation involving a negative-feedback loop.

KEY WORDS: *Strongylocentrotus purpuratus*, QPCR, Endomesoderm, Sea urchin larval development, Hindgut specification, GRN, Triple in situ hybridization

INTRODUCTION

The sea urchin embryo is a powerful developmental system that has been used to study embryological processes at many levels, from mechanisms of fertilization (e.g. Briggs and Wessel, 2006; Parrington et al., 2007) to gastrulation (e.g. Ettensohn, 1984; Hardin, 1996) and cell specification (e.g. pigment cells) (Calestani et al., 2003). In the recent era of molecular biology, the purple sea urchin *Strongylocentrotus purpuratus* has come to the forefront as the model urchin. *S. purpuratus* is the first non-chordate deuterostome to have its genome sequenced (Sea Urchin Sequencing Consortium, 2006), and is the taxon used in building of one of the first and most fully resolved gene regulatory networks that describes the genetic basis behind the separation of the germ layers from fertilization through gastrulation (Davidson et al., 2002).

One of these germ layers is the endoderm, which eventually gives rise to a three-part gut consisting of an esophagus, stomach and hindgut or intestine. Evidence of patterning is obvious in the dynamic expression of transcription factors within the endodermal tube (GataE, Brn 1/2/4, Fox A, Blimp/KroxA, Cdx and xLox, Hox11-13b) (Lee and Davidson, 2004; Yuh et al., 2005; Olivieri et al., 2006; Livi et al., 2006; Arnone et al., 2006; Arenas-Mena et al., 2006), as well as from some well-known endodermal marker genes (Endo1, Endo16, CyIIa) (Wessel and McClay 1985; Ransick et al., 1993; Arnone et al., 1998). Although the early specification of the gut results from the coordinated activity of the endomesodermal regulatory network genes, little is known about the later patterning events leading to the differentiation of three morphologically and functionally distinct gut regions.

[1]Stazione Zoologica Anton Dohrn di Napoli, Villa Comunale, 80121 Napoli, Italy.
[2]Department de Genètica, Universitat de Barcelona, Avenida Diagonal, 645, 08028 Barcelona, Spain.

*These authors contributed equally to this study
†Author for correspondence (e-mail: miarnone@szn.it)

Accepted 9 December 2008

In vertebrates, regionalization of the gut has been shown to be under the late control of homeobox genes, in particular the members of the so-called ParaHox class. The genes are called *gsx*, *xLox* and *cdx* in chordates, where the three have been identified (Brooke et al., 1998). In insects only orthologs of *gsx* (*ind*) and *cdx* (*caudal*) are known (Weiss et al., 1998; Mlodzik et al., 1985), whereas an *xLox* homolog has been identified in both annelids (Fröbius and Seaver, 2006; Kulakova et al., 2008) and mollusks (Barucca et al., 2006), as well as from the more basal nermertodermatida (Jimenez-Guri et al., 2006). Though ParaHox genes have been identified in several taxa, very little is known about the functions of this group of genes during development with the exception of the mouse homolog *Pdx1*, which plays an important role in pancreas formation (for a review, see Al-Quobaili and Montenarh, 2008).

SpLox, the purple urchin xLox homolog, is expressed in the mid- and hindguts of gastrula stage embryos, and is restricted to the posterior sphincter separating these two gut regions in the pluetus larva (Arnone et al., 2006). This expression pattern is conserved also in sea stars (R. Annunziata, unpublished) (Hwang et al., 2003). Given the relative simplicity of the sea urchin digestive system and the wealth of data available concerning the gene regulatory network (GRN) specifying the endodermal precursors, the purple urchin represents an optimal developmental system with which to investigate the role of ParaHox genes in endodermal partitioning to create a functional tripartite gut. Here, we describe our detailed analysis of the expression and function of the sea urchin *SpLox* gene and its genetic interaction with a second endodermally expressed ParaHox gene, *SpCdx*.

MATERIALS AND METHODS

Animals

Adult *Strongylocentratus purpuratus* were obtained from the Kerchoff Marine Laboratory, Corona del Mar USA, and housed in circulating sea water aquaria at the Stazione Zoologica Anton Dohrn, Naples, Italy. Spawning was induced by intracoelomic injection of 0.5 M KCl and embryos were kept in a temperature-controlled incubator (15°C), cultured in filtered seawater diluted 9:1 with de-ionized water.

Whole-mount in situ hybridization

Embryos and larvae were collected as needed and fixed for 2 hours to overnight in 4% paraformaldehyde in filtered seawater, washed in Tris-buffered saline (TBS) and stored in 70% ethanol until use. For detailed expression analysis of the onset of *SpLox* and *SpCdx* expression, a series of embryos was fixed every 2 hours between 48 and 72 hours post fertilization (hpf). Labeled probes were transcribed from linearized DNA using digoxygenin-11-UTP or fluorescein-12-UTP (Roche), or labeled with DNP (Mirus Cat # MIR 3800) following kit instructions. In situ RNA probe sequences are as previously published (*SpCdx*, *SpLox*) (Arnone et al., 2006) *Endo16* (Ransick et al., 1993). For single gene expression, the protocol outlined by Minokawa et al. (Minokawa et al., 2004) was followed. For multi-gene fluorescent in situ (up to three genes contemporaneously), fixed embryos were washed in Tris-buffered saline containing 0.1% Tween-20 (TBST), pre-hybridized for 1 hour at 65°C in fresh hybridization buffer (50% formamide, 5× SSC, 0.1% Tween-20, 50 μg/ml heparin, and 50 μg/ml yeast tRNA) and incubated overnight at 65°C with antisense labeled probes. Embryos were washed in a descending gradient of SSC (2×, 0.2×, 0.1×) at 65°C followed by TBST washes at room temperature. Embryos were then blocked for 30 minutes in fresh 0.5% Perkin Elmer Blocking Reagent (PEBR) in TBST, and incubated overnight at 4°C with peroxidase conjugated antibodies (Roche: 1 μl in 100 μl of 0.5% PEBR in TBST). Antibodies were removed with washes in TBST, and signal was developed with fluorophore-conjugated tyramide (1 μl/50 μl reagent dilutant: Perkin Elmer). Residual enzyme activity was inhibited via a 20-minute incubation in 0.1% hydrogen peroxide, followed by TBST washes prior to addition and development of the second and third antibody. Embryos were imaged with a Zeiss Axio Imager.M1. Triple in situs were imaged with a Zeiss 510Meta confocal microscope.

Morpholino antisense oligonucleotide (MASO) injections

We followed the method indicated by Oliveri et al. (Oliveri et al., 2003). All morpholino antisense oligonucleotides (MASOs) were used in a concentration of 150 μM. To assess the effect of morpholino injections, fertilized eggs were injected with the injection solution (1% rhodamine dextran in 0.1 M KCl) without morpholino oligonucleotides, or with one of the following control morpholinos: GeneTools standard control oligonucleotide, SpLox mutated morpholino sequence (mismatch control, see below), or a GCM specific morpholino that blocks pigment formation (Ransick and Davidson, 2006). We see no phenotypic effect upon injection of control morpholinos, and endoderm development is unaffected in the presence of GCM-MASO (see Fig. S1F in the supplementary material). Two different *SpLox* specific MASOs were used in combination with a mismatch control morpholino:

mLox1, AGTACcCGcGATTcTTCCcTTCgAT (mismatch control);
Lox1, AGTACGCGGGATTGTTCCCTTCCAT;
Lox2, AGGACATTGGATATTCAGACGCCAT.

The mismatch control morpholino produced no morphological phenotype (see Fig. S1I in the supplementary material), and was unable to block in vitro synthesis of SpLox protein (performed as described below under EMSA), which was completely inhibited by the Lox1 MASO (see Fig. S1J in supplementary material). No significant difference in phenotype was observed between Lox1 and Lox2 MASOs, and all data presented herein derives from the MASO directed against the 5′ start codon (Lox1). After injection, fertilized eggs were washed with fresh filtered seawater (FSW) and incubated overnight. The following day, rhodamine-positive embryos were transferred to new plates and incubated at 15°C in fresh FSW.

Assay on digestive function

One-week-old larvae were cultured for 6 days in the presence of the micro alga *Isochrysis galbana* (210^6 cell/ml). At different time points, larvae were selected and observed under a fluorescent microscope using a FITC filter set. The presence of chlorophyll in this phytoplankton species allows direct observation of the micro alga under fluorescent light, and allows for differential detection between degraded and intact algal cells. To assess levels of alkaline phosphatase in the guts of injected versus control larvae, alkaline phosphatase staining was performed as detailed by Livingston and Wilt (Livingston and Wilt, 1989).

Phalloidin and Endo1 immunostaining of embryos

Larvae were freshly fixed in 4% PFA in FSW for 2 hours at room temperature, washed multiple times in phosphate-buffered saline with 0.1% Tween-20 (PBST), and incubated overnight at 4°C with anti-Endo1 primary antibody (Wessel and McClay, 1985), diluted at working concentration (1:5) in 5% goat serum in PBST. Following primary antibody incubation, larvae were washed three times with PBST, and incubated for 1 hour at room temperature with the secondary antibody Alexa Fluor 555 goat anti-mouse IgG (Molecular Probes) diluted 1/100 in 5% goat serum in PBST. After removal of secondary antibodies, larvae were incubated in 1 μl phalloidin-488 in 100 μl PBST for 1 hour (Roche). Larvae were washed in PBST and mounted for imaging with a confocal microscope (Zeiss 510Meta).

Quantitative PCR (qPCR)

Total RNA was collected from a minimum of 400 larvae per experimental trial using a RNAeasy mini-kit (Qiagen) following the manufacturer's instructions. cDNA was synthesized with Sprint PowerScript (Clontech). qPCR was performed according to Rast et al. (Rast et al., 2002), using an ABI prism 7000 sequence detection system and SYBR green chemistry (PE Biosystems). For all qPCR experiments, the data from each cDNA sample were normalized against ubiquitin mRNA levels, which are known to remain relatively constant during embryogenesis (Nemer et al., 1991). Details of primer sets can be provided on request.

Electrophoretic mobility shift assay (EMSA)

Putative binding sites were identified by alignment of the Endo16 regulatory sequence (Yuh et al., 1994) with the *Pdx1*-binding sequence A1 from the insulin promoter (Liberzon et al., 2004). Of the putative sites found, we chose to analyze the most proximal one, which contains two core homeobox DNA-binding sites (site n. 28) (Yuh et al., 1994). Mobility shift assays were performed as previously described (Martin et al., 2001). In vitro translated SpLox protein was synthesized using the TNT coupled in vitro transcription/translation system (Promega) from the cDNA clone p16I16ES under the control of a T7 promoter. DNA-protein complexes were resolved by gel electrophoresis and imaged on a Typhoon Trio (Amersham).

RESULTS

Endodermal expression of *SpLox*

The spatial pattern of *SpLox* expression at 72 and 96 hours has been previously reported (Arnone et al., 2006). We have further characterized the detailed spatial expression pattern from pre-gastrula through 72 hours by whole-mount in situ hybridization, as illustrated in Fig. 1.

At the mesenchyme blastula stage (Fig. 1A), *SpLox* transcripts are not detectable, consistent with the limited number of transcripts per embryo detected by quantitative PCR (Arnone et al., 2006). The first developmental stage at which the signal is clearly visible is the late mid-gastrula, when the archenteron is more than three-quarters invaginated. At this stage, expression is first seen within single cells at the edge of the blastopore (Fig. 1B). The onset of this expression pattern is consistently asymmetrical; however, within 2 hours, all cells surrounding the inner edge of the blastopore exhibit high levels of expression (Fig. 1C). The original asymmetric pattern of expression appears to be retained, with an expanded signal localized in the aboral side as the archenteron elongates (Fig. 1D,E). When gastrulation is completed, the domain of *SpLox*-expressing cells encompasses the entire posterior region of the developing gut (Fig. 1F). As differentiation of the tripartite gut continues, expression within the hindgut is reduced and expression becomes restricted to the constriction between the mid- and hindgut (Fig. 1G,H). This endodermal pattern is stable, and persists at least into the pluteus stage, although at lower levels (Fig. 1I).

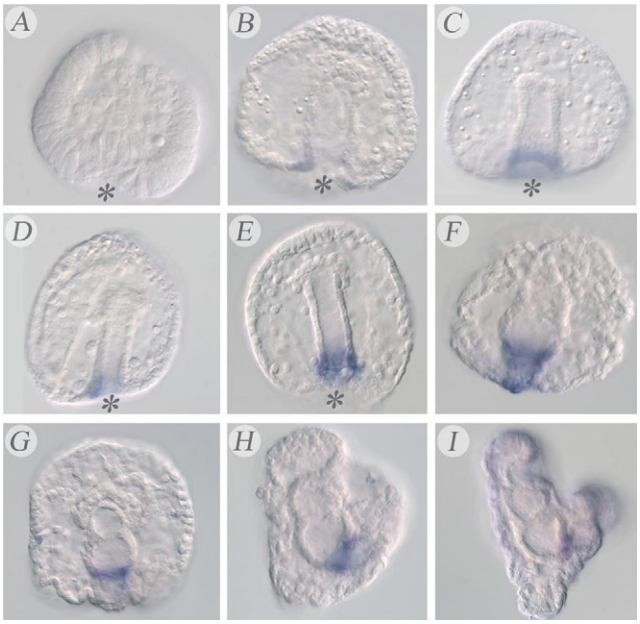

Fig. 1. Expression pattern of the *SpLox* gene from blastula through pluteus larva in *Strongylocentrotus purpuratus*. (**A**) Mesenchyme blastula showing no *SpLox* expression. (**B**) Midgastrula. First detectable expression appears in cells on one side of the blastopore (*). (**C-E**) Mid to late gastrula. Expression is detected in all cells surrounding the blastopore and the posterior-most endodermal tube. (**F**) End of gastrulation: prism stage larva. The entire posterior endodermal tube exhibits *SpLox* expression, from the posterior midgut through to the anus. (**G**,**H**) Early pluteus larva collected 4 hours after that shown in F shows expression restricted to the posterior midgut/hindgut boundary. (G) Oral view; (H) lateral view, oral end upwards. (**I**) 72-hour pluteus larva, in lateral view, oral end upwards. Expression is retained at the posterior sphincter.

SpLox-MASO injections disrupt gut morphology

To investigate the function of the *SpLox* gene in the embryo, gene-specific morpholino antisense oligonucleotides (MASO) were injected into fertilized eggs to silence the gene by blocking production of the protein, and the phenotype of the resultant embryos and larvae was analyzed. Control injected larvae show no phenotypic effects (see Fig. S1 in the supplementary material). Injection of the SpLox-MASO results in alterations of endoderm formation, as expected from the in situ expression pattern. The ectoderm develops normally and the secondary mesenchyme derivatives are both differentiated and properly distributed (e.g. the pigment cells are located mainly in the aboral ectoderm). The formation of the vegetal plate and invagination of the archenteron are not affected (data not shown) in accordance with the in situ hybridization data, indicating that *SpLox* is not expressed until mid-late gastrula in *S. purpuratus*. The first and most apparent morphological difference between control (Fig. 2C) and morpholino (Fig. 2F) -injected embryos is the delay in development of the constriction between the midgut and hindgut (see also Fig. S1 in the supplementary material), corresponding to the late expression domain of this gene. Embryos are not able to compensate for this loss, as evidenced by the continued absence of a closed sphincter in stage I (Smith et al., 2008) pluteus larvae (compare Fig. 2A,B with 2D,E). The tripartite gut can be clearly identified in control injected specimens (rhodamine dextran-KCl injected; Fig. 2A,B): foregut, midgut and hindgut are clearly defined by the presence of an anterior and posterior sphincter separating the midgut from the foregut and hindgut, respectively, whereas SpLox-MASO injected embryos have an anterior cardiac sphincter (gray arrows in Fig. 2D,E) but show only a mild posterior constriction (white arrows). We further investigated the lack of this posterior sphincter using FITC-labeled phalloidin to visualize actin fibers, and analyzed the larvae with a confocal microscope to ensure accurate interpretation of the staining patterns. Control animals have a well-delineated border between the gut compartments, including a muscular sphincter (Fig. 2G-J). SpLox-MASO-treated embryos lack this sphincter, possessing solely a mild posterior constriction (Fig. 2K-N). In addition, the entire mid and hindgut region exhibits staining of short processes within the lumen (arrowheads in Fig. 2N) that are not seen in control larvae (Fig. 2J). Surprisingly, we find that morpholino-injected embryos also exhibit a reduction in the organization of the muscle fibers surrounding the foregut. In order to investigate whether these effects are species specific, we also tested the morphological effects of this morpholino in another distantly related sea urchin species, *Paracentrotus lividus*. We find that these morpholino-injected embryos also lack the posterior sphincter and exhibit a disorganized foregut musculature (data not shown), suggesting a conserved gene function within the echinoids.

The digestive functions of SpLox-MASO injected embryos are inhibited

In addition to the morphological effect, the absence of SpLox function alters the digestive properties of the embryonic gut. We analyzed food ingestion in mutant and control larvae by regularly feeding animals with a culture of single-celled alga, *Isochrysis galbana*, starting at 72 hours of development. The passage of food along the gut cavity is easily detected owing to the transparency of the embryonic wall and to the fluorescent signal of the microalga with which the larvae are fed. Whereas in control larvae the algal cells are degraded and ingested by the intestinal cells, in the SpLox-MASO injected larvae the algal cells remain intact and are excreted without further degradation (Fig. 3A,B,D,E). Further evidence for loss of digestive capacity within the gut of MASO-injected larvae is the reduction of the activity of a gut-specific enzyme, alkaline phosphatase (Livingston and Wilt, 1989), as demonstrated by a reduction in phosphatase activity within the gut (Fig. 3C,F).

Levels of endoderm marker genes are altered in the absence of *SpLox* function

To address the genetic mechanism by which *SpLox* exerts its effect, we evaluated changes in the levels of transcription in morpholino-injected larvae 72 and 96 hours post-fertilization using quantitative PCR. Transcript levels were evaluated for some endoderm transcription factors from the endomesoderm gene regulatory network (GRN), endodermally expressed ParaHox genes, a number of transcription factors known to be involved in the putatively homologous network derived from studies of the xLox homolog (*Pdx*) in the vertebrate pancreas, as well as a number of terminal differentiation genes (Fig. 4). Only those genes whose transcript levels differ by a factor of ±1.8 are considered to be significant (see bold text in Fig. 4). Genes from the endomesoderm GRN, which are expressed much earlier in development than *SpLox*, show no significant changes in transcript levels, with the exception of brachyury (*brac*), the expression of which increases by a moderate twofold, in three out of five replicate experiments (Fig. 4). By contrast, significant changes in transcript levels were identified for both *SpLox* itself, as well as for the other endodermally expressed ParaHox gene *SpCdx*. *SpLox* transcript levels increase by 2-7 times

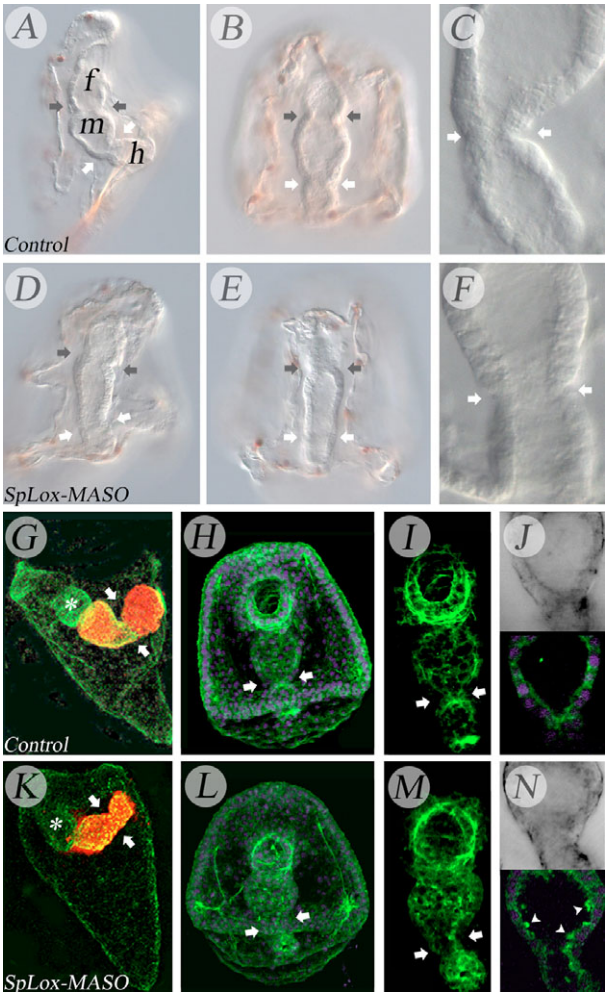

Fig. 2. Morphological phenotype resulting from disruption of SpLox in *Strongylocentrotus purpuratus*. (**A**,**B**) Stage I pluteus larvae developed from rhodamine dextran-KCl-injected eggs show a well-defined tripartite gut with anterior (gray arrows) and posterior (white arrows) sphincters separating the midgut (m) from foregut (f) and hindgut (h), respectively. (A) Lateral and (B) oral views. (**D**,**E**) SpLox-MASO injected larvae show disorganized structure of the endodermal epithelia and are missing the posterior sphincter between the midgut and hindgut (white arrows), exhibiting only a mild posterior constriction of the gut. (D) Lateral and (E) oral views. Gray arrows indicate anterior sphincter (**C**,**F**) Posterior regions of the developing gut from prism stage larvae, wherein the distinct reduction of the posterior constriction (white arrows) is first apparent in SpLox-MASO-injected embryos (F) compared with control injected embryos (C). (G-I,K-M) Three-dimensional maximal projection of confocal image stacks from phalloidin stained (green) control (G-I) and SpLox-MASO (K-M) injected larvae. (**G**,**K**) Lateral view of a stage I pluteus larva showing staining of the midgut and hindgut by an Endo1 antibody (red). Note the muscle fibers that define the foregut anteriorly (*) in the control larva (G) and are less conspicuous in the experimental larva (K). (**H**,**L**) Oral views, phalloidin staining (green) with nuclear counterstain (purple). (**I**,**M**) Reconstructions of phalloidin staining in endoderm from the same larvae imaged in H and L. Phalloidin fibers collect at the level of the midgut-hindgut sphincter (white arrows) and are present in the control larvae G-I, but are absent from SpLox-MASO injected larvae K-M. (**J**,**N**) A single optical section from the same larvae shown in H,I and L,M taken at the level of the midgut-hindgut junction; bright-field above, fluorescence below. The smooth surface of stomach lumen in control (J) when compared with the SpLox-MASO larva (N) where many phalloidin-positive projections are evident (white arrowheads).

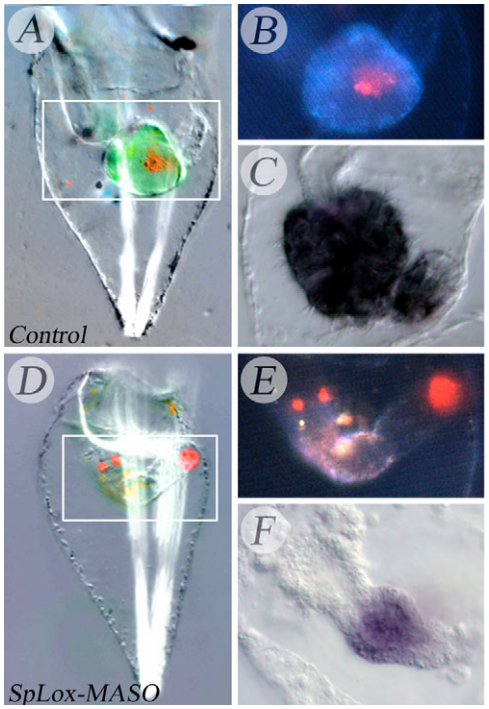

Fig. 3. Silencing of *SpLox* results in disruption of feeding abilities in *Strongylocentrotus purpuratus* larvae. (A-C) Control MASO-injected (D-F) and SpLox-MASO-injected larvae. (**A**,**D**) Bright-field images with overlaid fluorescence excited through a 488 wavelength filter showing degraded chlorophyll (green) and intact algal cells (red). (**B**,**E**) Higher magnification of the gut of the same larvae shown in A,D imaged under UV excitation to illustrate degraded (blue) and intact (red) chlorophyll. Control injected larvae (A,B) show incorporation of chlorophyll within the midgut, whereas SpLox-MASO injected larvae (D,E) show only undigested algal pellets within the digestive tract. (**C**,**F**) Alkaline phosphatase staining. The control injected larva imaged in C shows high levels of alkaline phosphatase activity when compared with the SpLox-MASO-injected larva imaged in F.

over the levels in control embryos at both time points, whereas *SpCdx* transcript levels decrease 2-5 times at both time points when compared with control embryos. Two genes identified as being part of the murine Pdx1 pathway, the islet factor 1 gene (*Isl1*) (Kojima et al., 2002) and myelin transcription factor 1 gene (*Myt1*) (Gu et al., 2004), are the only other transcription factors examined that demonstrate altered expression in response to silencing the *SpLox* gene.

Terminal differentiation genes displayed much greater responses to the silencing of *SpLox*. Both endodermal markers examined demonstrate significant changes in transcriptional expression. Consistent with the decrease in enzyme activity in injected larvae (see Fig. 3C,F), alkaline phosphatase (*ap*) transcripts decrease, whereas *Endo16* levels increased. By contrast, a mesodermal terminal differentiation marker, *capk* (Rast et al., 2002), showed little change in transcript prevalence. Also consistent with the morphological phenotype, wherein there is a disruption of the organization of the musculature associated with the gut (see Fig. 2), a second mesodermal differentiation marker, actin M (*actM*) (Cox et al., 1986), consistently decreased in expression (two- to fivefold decrease), as did a sea urchin muscle-specific transcription factor (*sum1*, a MyoD-like gene) (Beach et al., 1999).

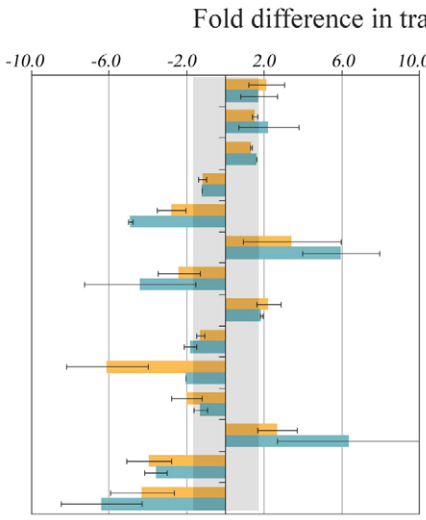

gene	72 hpf	96 hpf
brac	**2.5**; **2.8**; 1.0	**2.4**; 1.0
foxA	1.6; 1.6; 1.3	**3.3**; 1.1
foxB	1.3; 1.3	1.6; 1.6
hox11/13b	-1.1; -1.4; -1.0	-1.2
cdx	**-2.9**; **-3.5**; **-2.0**	**-5.0**; **-4.9**
lox	**2.1**; **6.3**; **1.8**	**7.3**; **4.5**
isl	**-3.2**; **-1.8**; **-3.5**; -1.2	**-6.4**; **-2.4**
myt	**2.7**; **1.8**	**1.9**; **1.8**
unc	-1.4; -1.2	-1.6; **-2.0**
ap	**-9.1**; **-3.1**	**-2.1**
capk	**-1.9**; -1.4; **-3.1**; -1.6	-1.1; -1.5
endo16	1.7; **3.7**; **2.5**	**9.0**; **3.7**
actM	**-4.4**; **-5.3**; **-3.4**; **-2.7**	**-3.2**; **-4,0**
sum1	**-5.8**; **-4.6**; **-2.5**	**-4.9**; **-7.9**

Fig. 4. Changes in gene expression levels assessed by qPCR in SpLox-MASO-injected *Strongylocentrotus purpuratus* larvae when compared with levels in control injected larvae. Total RNA was collected from control and SpLox-MASO injected larvae at two time points [72 (yellow) and 96 (green) hours post fertilization]. Experiments were repeated at least twice, with replicates from different batches separated by semicolons. Data are expressed as a fold difference from control larvae and are illustrated graphically on the left, with the numerical data presented on the right. We assume an amplification efficiency of 1.9, and all samples varied from one another by no more than 0.3 cycles. For all data, the cycle threshold (C_T) was first normalized to ubiquitin expression levels in each sample. Fold difference is calculated as $1.9^{\Delta Ct}$; thus, fold differences greater than ±1.8 (gray) are considered significantly different and are in bold. Genes of the endomesodermal GRN are presented first, followed by the two ParaHox genes, genes that were chosen because of their role in the pancreatic GRN in vertebrates, downstream structural genes from the echinoderm endomesodermal GRN and, finally, two genes involved in muscle development. We find no differences in expression of endomesodermal GRN genes, assumed to be upstream from *SpLox*, whereas two transcription factors from the vertebrate pancreas network show altered levels of expression (*isl* and *myt*), as do the endodermal structural genes (*Endo16* and *ap*) and those involved in muscle formation (*actM* and *sum1*).

SpLox represses *Endo16* expression in the hindgut

Endo16 is an extremely well-studied endodermal marker gene, encoding a calcium-binding protein (Soltysik-Española et al., 1994) that is initially expressed throughout the vegetal plate and invaginating endoderm. However, at the end of gastrulation, its expression is restricted to the midgut (Ransick et al., 1993). The early domain of *SpLox* expression almost completely overlaps with the posterior-most expression domain of *Endo16* (Fig. 5A,B). Our qPCR data indicate that the transcript levels of *Endo16* are highly elevated in response to silencing *SpLox*. Thus, we investigated whether this increase corresponds to a change in the *Endo16* expression domain or simply an upregulation of the gene within the confines of its normal expression area. Expression levels of *Endo16* are consistently elevated in injected embryos; *Endo16* transcripts are detectable by in situ hybridization in less than half the time it takes for the in situ signal to develop in control embryos processed in parallel (data not shown). Furthermore, we find that the domain of *Endo16* expression is expanded to encompass the entire mid- and hindgut territories (Fig. 5E,F), whereas expression of this gene in control larvae is confined to the midgut region (Fig. 5C,D). This expansion of the expression domain remains restricted to the endoderm; at no time is ectopic expression of *Endo16* outside of the gut observed. This expression pattern is also retained in 1-week-old stage I pluteus larvae (data not shown).

The *Endo16* gene possesses one of the most thoroughly studied cis-regulatory regions (Yuh et al., 1998). Owing to the strong effect of the SpLox morpholino injections on Endo16 expression, we investigated its cis-regulatory sequence for possible SpLox-binding sites. We analyzed the proximal-most putative binding sequence (Fig. 6A) by competitive binding assay, using in vitro synthesized SpLox and oligonucleotides containing this sequence. We find that SpLox specifically binds this oligonucleotide (Fig. 6B, lane 1), as assessed by competition with increasing concentrations of unlabeled oligonucleotide (Fig. 6B, lanes 2,3). By contrast, addition of unlabeled oligonucleotides containing a mutation within the ATTA core binding sequence (Fig. 6A) does not interfere with the efficiency of in vitro binding (Fig. 6B, lanes 4,5), indicating the specificity of the binding to that site. Additionally, we show that in vitro synthesized SpLox also binds with high efficiency to oligonucleotides containing the Pdx1-binding site A1 from the insulin promoter (Liberzon et al., 2004) (Fig. 6B, lanes 6,7).

Posterior endodermal patterning results from interaction between ParaHox genes

One of the most intriguing results from the qPCR analysis is the decrease in expression of a second ParaHox gene expressed in the gut: the caudal homolog *SpCdx*. In order to address the interactions between these two genes, we re-evaluated the expression pattern of the *SpCdx* gene at the same level of detail as that of *SpLox*. *SpCdx* expression appears slightly later than *SpLox* expression (Fig. 7A,B), but similarly appears as cells enter the blastopore near the end of gastrulation (Fig. 7C,D). *SpCdx* expression is retained throughout the developing hindgut region (Fig. 7E,F), and persists at high levels in the hindguts of 72-hour pluteus larvae (Fig. 7G-I). To investigate the extent of overlapping expression between these two genes, we performed double-fluorescent in situ hybridization. We find that at the onset of *Cdx* expression, the expression domains of these two genes largely overlap (Fig. 8A-C). As development progresses, *SpLox* progressively clears from the hindgut region (Fig. 8D-F) so that the fully developed larva retains *SpCdx* expression throughout the hindgut, whereas *SpLox* is restricted to the posterior sphincter in a non-overlapping domain of expression (Fig. 8G-I).

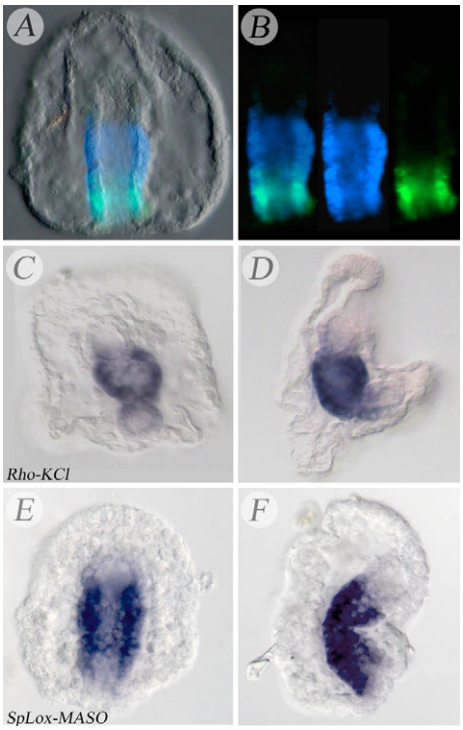

Fig. 5. *SpLox* clears expression of the endoderm gene *Endo16* from the hindgut region. (**A**,**B**) Co-expression of *Endo16* (blue) and *SpLox* (green) in a late gastrula stage embryo showing the overlapping domains of expression (blue-green). The fluorescent channels are shown separately in B. (**C**,**D**) *Endo16* expression in control pluteus larvae is restricted to the midgut; (C) oral and (D) lateral view. (**E**,**F**) *Endo16* expression is expanded into the hindgut region in SpLox-MASO injected pluteus larva. (E) Oral and (F) lateral views.

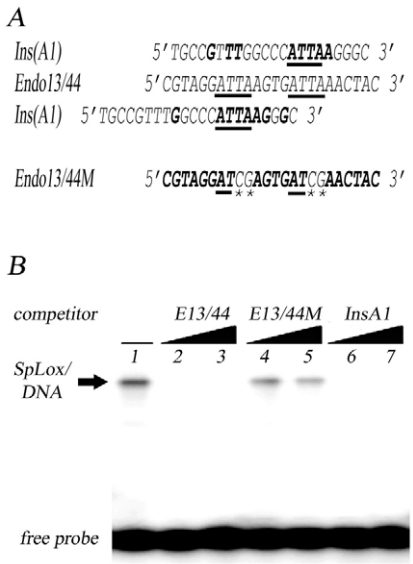

Fig. 6. *SpLox* binds to the regulatory region of *Endo16* in vitro. (**A**) Sequences used for the binding assay shown in B (see Materials and methods for details of origin of these sequences). The core homeobox DNA-binding site is underlined, and nucleotide alignment of the A1 Pdx-binding site of the insulin promoter (*InsA1*) (Liberzon et al., 2004) with two putative Lox-binding sites included in the Endo16 13/44 promoter element (*Endo13/44*) (Yuh et al., 1994) are shown in bold. Altered nucleotides in the mutated oligonucleotide (*Endo13/44M*) are indicated (*). (**B**) In vitro binding assay of synthesized SpLox protein shows effective binding to putative Lox-binding site from the *Endo16* promoter (lane 1). Binding to labeled oligonucleotides is reduced in the presence of increasing concentration (50 and 100-fold molar excess) of unlabeled competitor DNA (*E13/44*; lanes 2,3), whereas binding efficiency is unchanged if the competing unlabeled oligonucleotide contains a mutation (*E13/44M*; lanes 4,5). The SpLox protein binding is also effectively inhibited by competition with unlabeled oligonucleotides containing the A1 Pdx1-binding site from the insulin promoter (*InsA1*; lanes 6,7).

By contrast, SpLox-MASO injected larvae show a distinct absence of *SpCdx* expression within the hindgut (Fig. 8L), in accordance with the decrease in the transcripts of this gene indicated by qPCR. The absence of *SpCdx* expression suggests that SpLox is involved in *SpCdx* activation in the zone of overlapping expression. We also find that *SpLox* expression is no longer restricted to the posterior sphincter, as in control larvae, but rather maintained within the entire posterior-most region of the developing gut in the SpLox-MASO-injected animals (Fig. 8J,K). This result is consistent with the elevated *SpLox* transcript levels revealed by qPCR (see Fig. 4), and together illustrate that translation of SpLox is required for inhibiting further transcription of this gene within the region of the hindgut.

DISCUSSION

SpLox is necessary for establishing the boundary between the stomach and intestine

During organogenesis, multiple cell types are generated and organized into elaborate structures. This process depends on the exquisite coordinated activity of genes and gene networks, to ensure that the final pattern and functionality of the organ is properly achieved. Using gene knockdown, in situ hybridization and quantitative PCR analyses, we have provided data supporting the hypothesis that ParaHox genes are essential in the regional endodermal patterning leading to a functional gut. In the absence of SpLox protein translation, mutant embryos demonstrate an anterior-posterior identity shift, wherein the midgut marker *Endo16* is expanded posteriorly, *SpLox* expression is maintained posteriorly throughout the presumptive hindgut region, and the hindgut marker *SpCdx* is extremely reduced or absent. A similar phenotype in a distantly related urchin species, *Paracentrotus lividus* (data not shown), supports the notion that the results presented here hold not only for the sea urchin *S. purpuratus*, but also for echinoid echinoderms as a group. The *SpLox* phenotype described here is similar to that observed in mice lacking the murine homolog *Pdx1*. In these mice, the rostral duodenum is malformed with a misshapen pyloric sphincter, leading to deficiencies in gastric emptying, and the anterior duodenum resembling a posterior extension of the stomach (Jonsson et al., 1994; Offield et al., 1996). Thus, consistent with our data from echinoid echinoderms, the boundary between expression domains of murine gastric and duodenal markers appear shifted posteriorly. Pdx1 also acts as a potent repressor of posterior gut enzymes, including those normally mediated by Cdx homologs (Heller et al., 1998; Wang et al., 2004). Taken altogether, these data clearly indicate the importance of SpLox in establishing the mid-hindgut boundary within the deuterostome lineage.

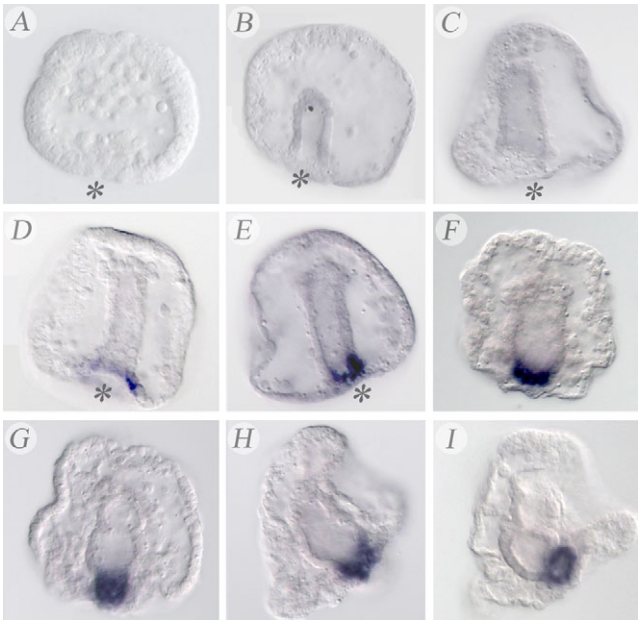

Fig. 7. Expression pattern of the *SpCdx* gene from blastula through pluteus larvae in *Strongylocentrotus purpuratus*. Embryos correspond to the same batch as those shown in Fig. 1 for *SpLox* expression. (**A-C**) Mesenchyme blastulae through mid-late gastrulae show no *SpCdx* expression. (**D**) Late gastrula. First detectable expression appears in cells surrounding the blastopore (*). (**E**) Late gastrula. Expression is detected in all cells surrounding the blastopore and the posterior-most endodermal tube. (**F**) End of gastrulation: prism stage larva shown in oral view. The posterior-most endodermal tube exhibits *SpCdx* expression. (**G**,**H**) Early pluteus larvae collected 4 hours after that shown in F show continued high levels of expression throughout the hindgut region. (G) Oral view; (H) lateral view. (**I**) 72-hour pluteus larva in lateral view showing retention of the high expression levels throughout the hindgut.

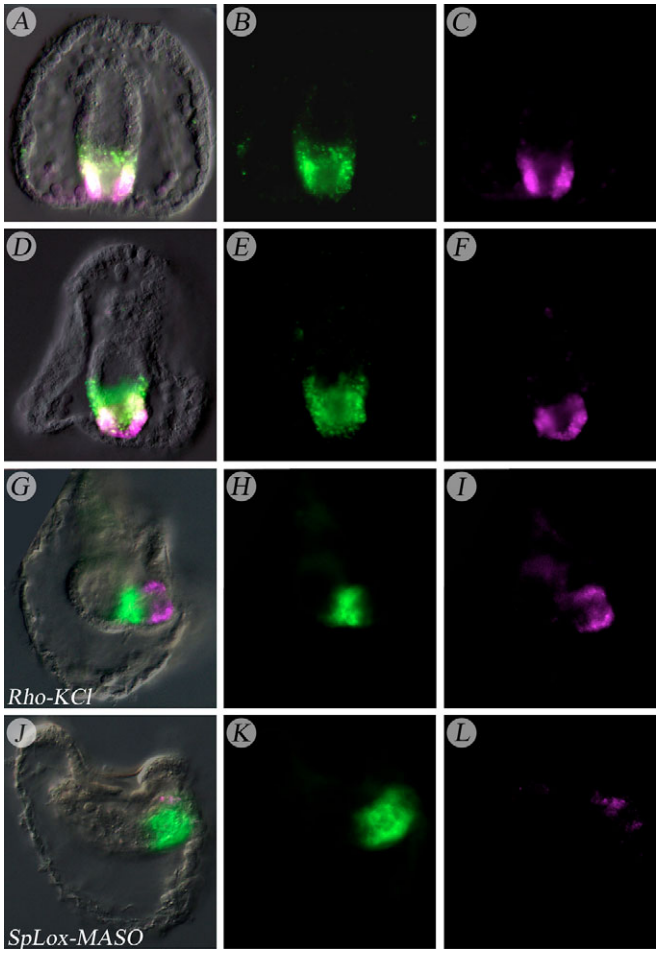

Fig. 8. ParaHox genes *SpLox* and *SpCdx* interact to regulate hindgut formation, as illustrated with double in situ hybridization. (A,D,G,J) Embryos photographed using DIC imaging, with the fluorescent gene expression patterns overlaid, overlapping expression appears white. (B,E,H,K) The green channel only (*SpLox* expression). (C,F,I,L) The red channel (*SpCdx* expression). (A-I) Double in situ of expression domains in normal embryos. (J-L) Double in situ illustrating expression domains in SpLox-MASO-injected embryos. (**A-C**) Late gastrula stage embryo showing largely overlapping expression domains of both genes, although the *SpLox* domain extends further anteriorly (green), and the *SpCdx* domain extends further posteriorly (purple). (**D-F**) Prism stage larva showing a greater region of non-overlapping expression domains. (**G-I**) Control injected pluteus larva showing mutually exclusive, non-overlapping expression domain for both genes. (**J-L**) Pluteus larva developed from an egg from the same batch as the larva shown in G-I, injected with the SpLox-MASO. *SpLox* expression is maintained throughout the hindgut (K) when compared with control (G,H), whereas *SpCdx* is absent in the posterior hindgut in injected larvae (L) compared with control (I).

Hox genes are known for their coordinated control of patterning of body regions, for example rhombomere patterning under the control of Hoxb genes (Maconochie et al., 1997). Little is known, however, about whether ParaHox genes also function in a coordinated manner to establish boundaries between adjacent territories. Our results reveal that the silencing of an anteriorly expressed ParaHox gene (*SpLox*) leads to the loss of a posterior identity (hindgut), accompanied by the downregulation of a second ParaHox gene (*SpCdx*) that is normally expressed in the missing territory. These data suggest coordination between these two ParaHox genes at a gene regulatory level. Here, we present a proposal for a gene regulatory network involved in hindgut specification (Fig. 9), derived from the data described in this article.

We suggest a model of regulatory interactions with the following components:

(1) SpLox protein represses the expression of the midgut marker gene *Endo16* in the hindgut territory (see Figs 4 and 5). We suggest that this interaction may be direct, owing to the amplitude of *Endo16* response as assayed by qPCR (see Fig. 4), and to the fact that SpLox protein binds efficiently to a putative binding site within the *Endo16* promoter (see Fig. 5). We tested only the proximal-most putative binding site, leaving open the possibility that SpLox may bind also other more distal sites.

(2) SpLox protein activates the expression of *SpCdx* (see Fig. 4 and Fig. 8L). This activation occurs necessarily in concert with other hindgut specific regulatory genes, because *Cdx* is not activated throughout the entire *SpLox* domain. *Hox 11-13b* is a good candidate for one such gene, as it appears to be expressed in the same domain as *Cdx*. However, its expression is initiated much earlier in development. Knockdown of *Hox 11-13b* results in embryos that show a posterior expansion of Endo16 into the hindgut (Arenas-Mena et al., 2006), similar to the phenotype of SpLox morpholino

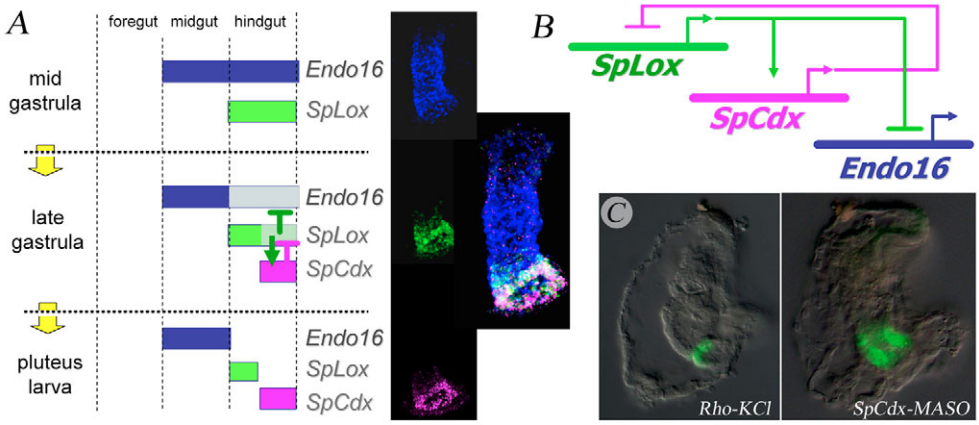

Fig. 9. Model of hindgut specification involving two ParaHox genes. (**A**) Summary of expression data for *SpLox*, *SpCdx* and the endodermal marker *Endo16*. Expression is shown schematically on the left, with confocal reconstruction of a triple in situ illustrating the expression of all three genes in a late gastrula stage embryo shown on the right. At the onset of *SpLox* expression in the late mid-gastrula stage embryo, *Endo16* is expressed throughout the presumptive mid and hindgut territories (blue). *SpLox* (green) represses the expression of *Endo16* in the area of overlapping expression, eliminating *Endo16* expression from the hindgut region. *SpCdx* (purple) expression begins in the posterior-most region of the endodermal tube, in the presumptive hindgut. We propose that *SpLox* is involved in the activation of *SpCdx* in this region, and that once activated *SpCdx* inhibits further expression of *SpLox* in the hindgut. (**B**) Gene network diagram summarizing these interactions. Repression of *Endo16* by *SpLox* is thought to be a direct interaction based upon the data presented in this paper. Interactions between *SpLox* and *SpCdx*, the two ParaHox genes, may be either direct or indirect. (**C**) Preliminary data showing the expression of *SpLox* (green) in embryos injected with a MASO targeting the donor splice site between the first and second *SpCdx* exons (5′-TAGCTTTTGGTTAAATACCTGTTT). SpCdx-MASO injected larvae (right) show expanded expression of *SpLox* into the hindgut when compared with control (*Rho-KCl*)-injected larvae (left).

embryos (see Fig. 5). Unfortunately SpLox was not analyzed in the *Hox11-13b* knockdown experiments, and, thus, we cannot speculate whether or not this similar phenotype is due to abolition of the SpLox protein.

(3) We propose that transcribed SpCdx protein acts as a repressor of *SpLox* in its posterior domain of expression. Silencing of *SpLox* leads to increase in SpLox transcripts (see Fig. 4) and retention of *SpLox* expression in the hindgut territory (see Fig. 8K), suggesting that SpLox protein initially activates a repressor in the hindgut territory that restricts *SpLox* expression to the level of the posterior sphincter (see Fig. 1G-I). *SpCdx* is expressed in this territory and is activated by SpLox protein (see Figs 4 and 7, and Fig. 8L). Furthermore, we have found that silencing *SpCdx* leads to a similar expansion of *SpLox* expression into the hindgut (preliminary data; Fig. 9C), supporting the supposition that SpCdx is involved in repressing *SpLox* in the hindgut.

These data add considerable strength to the hypothesis that a negative-feedback loop exists between these two ParaHox genes, and that this gene regulatory circuit is necessary for the establishment of hindgut territories. An ancestral function of caudal homologs in determining hindgut territories was first proposed based upon work in *Drosophila* (Wu and Lengyel, 1998). As our data illustrate, the sea urchin provides a precise example of how a developmental field (gut) is subdivided using homeobox genes and how these subfields are subsequently refined by a negative-feedback loop at the gene regulatory level.

Conclusions and perspectives

Our results are consistent with the view that gut morphogenesis in sea urchins has different temporal components: an early specification process (governed by the Wnt pathway) (Wikramanayake et al., 2004) and a late differentiation process in which genes of the ParaHox complex (*SpLox* and *SpCdx*) are involved in regionally partitioning the endoderm. The phenotypes generated through the use of gene specific MASOs have shown us that SpLox is a key regulator in the formation of the midgut-hindgut boundary, repressing regions of the midgut differentiation program and activating the hindgut gene battery through a second ParaHox gene, *SpCdx*.

SpLox endodermal expression conforms to the rule that *xLox* homologs are endodermal markers, expressed in specific regions within the gut and endodermal derivatives (Wright et al., 1989; Brooke et al., 1998; Stoffers et al., 1999; Fröbius and Seaver, 2006) and supports the speculation that the *SpLox* orthologs are part of a group of genes dedicated to generate diversity in the gut (Brooke et al., 1998; Fröbius and Seaver, 2006). Although no functional data are available from a protostome, the nested expression pattern of the endodermal ParaHox genes in annelids (Fröbius and Seaver, 2006; Kukalova et al., 2008) suggests a similar system of regionalization. This would imply that ParaHox gut regionalization is shared among all bilaterians, thus representing a pan-bilaterian character. Moreover, our data indicate that at least portions of the gene regulatory network that control pancreas development and maintenance in vertebrates were available for cooption from the gene regulatory network used to partition the gut of the common ancestor of the deuterostomes. It seems clear now that the ParaHox group of genes regionalizes the endoderm along the anteroposterior axis. Thus, given the apparent use of the same system in both deuterostomes and protostomes, we assume that this arose early in evolution, most probably coincidently with the origin of bilaterians.

This work was supported by grants from the Marine Genomics Europe Network of Excellence (GOCE-04-505403, GARNET project; M.I.A. and F.R.) and a fellowship of the Marie Curie RTN ZooNet (MRTN-CT-2004-005624; A.G.C.). The authors thank Dave McClay for the gift of the Endo1 antibody used in Fig. 2. They also thank Marco Borra and Elvira Mauriello of the Stazione Zoologica Anton Dohrn di Napoli Molecular Biology Service (SBM-SZN) for their assistance with qPCR and sequencing, and anonymous reviewers for useful comments regarding an earlier draft of the manuscript.

Supplementary material

Supplementary material for this article is available at
http://dev.biologists.org/cgi/content/full/136/4/541/DC1

References

Al-Quobaili, F. and Montenarh, M. (2008). Pancreatic duodenal homeobox factor-1 and diabetes mellitus type 2 (review). *Int. J. Mol. Med.* **21**, 399-404.

Arenas-Mena, C., Cameron, R. A. and Davidson, E. H. (2006). Hindgut specification and cell-adhesion functions of *Sphox11/13b* in the endoderm of the sea urchin embryo. *Dev. Growth Differ.* **48**, 463-472.

Arnone, M. I., Martin, E. L. and Davidson, E. H. (1998). Cis-regulation downstream of cell type specification: a single compact element controls the complex expression of the *Cylla* gene in sea urchin embryos. *Development* **125**, 1381-1395.

Arnone, M. I., Rizzo, F., Annunciata, R., Cameron, R. A., Peterson, K. J. and Martinez, P. (2006). Genetic organization and embryonic expression of the ParaHox genes in the sea urchin *S. purpuratus*: insights into the relationship between clustering and colinearity. *Dev. Biol.* **300**, 63-73.

Barucca, M., Biscotti, M. A., Olmo, E. and Canapa, A. (2006). All the three ParaHox genes are present in *Nuttallochiton mirandus* (Mollusca: polyplacophora): evolutionary considerations. *J. Exp. Zoolog. B Mol. Dev. Evol.* **306**, 164-167.

Beach, R. L., Seo, P. and Venuti, J. M. (1999). Expression of the sea urchin MyoD homologue, *SUM1,* is not restricted to the myogenic lineage during embryogenesis. *Mech. Dev.* **86**, 209-212.

Briggs, E. and Wessel, G. M. (2006). In the beginning...animal fertilization and sea urchin development. *Dev. Biol.* **300**, 15-26.

Brooke, N. M., Garcia-Fernandez, J. and Holland, P. W. (1998). The ParaHox gene cluster is an evolutionary sister of the Hox gene cluster. *Nature* **392**, 920-922.

Calestani, C., Rast, J. P. and Davidson, E. H. (2003). Isolation of pigment cell specific genes in the sea urchin embryo by differential macroarray screening. *Development* **130**, 4587-4596.

Cox, K. H., Angerer, L. M., Lee, J. J., Davidson, E. H. and Angerer, R. C. (1986). Cell lineage-specific programs of expression of multiple actin genes during sea urchin embryogenesis. *J. Mol. Biol.* **188**, 159-172.

Davidson, E. H., Rast, J. P., Oliveri, P., Ransick, A., Calestani, C., Yuh, C. H., Minokawa, T., Amore, G., Hinman, V., Arenas-Mena, C. et al. (2002). A provisional regulatory gene network for specification of endomesoderm in the sea urchin embryo. *Dev. Biol.* **246**, 162-190.

Ettensohn, C. A. (1984). Primary invagination of the vegetal plate during sea urchin gastrulation. *Amer. Zool.* **24**, 571-588.

Fröbius, A. C. and Seaver, E. C. (2006). ParaHox gene expression in the polychaete annelid *Capitella* sp. I. *Dev. Genes Evol.* **216**, 81-88.

Gu, G., Wells, J. M., Dombkowski, D., Preffer, F., Aronow, B. and Melton, D. A. (2004). Global expression analysis of gene regulatory pathways during endocrine pancreatic development. *Development* **131**, 165-179.

Hardin, J. (1996). The cellular basis of sea urchin gastrulation. *Curr. Top. Dev. Biol.* **33**, 159-262.

Heller, R. S., Stoffers, D. A., Hussain, M. A., Miller, C. P. and Habener, J. F. (1998). Misexpression of the pancreatic homeodomain protein *IDX-1* by the Hoxa-4 promoter associated with agenesis of the cecum. *Gastroenterology* **115**, 381-387.

Hwang, S. P., Wu, J. Y., Chen, C. A., Hui, C. F. and Chen, C. P. (2003). Novel pattern of *AtXlox* gene expression in starfish *Archaster typicus* embryos. *Dev. Growth Differ.* **45**, 85-93.

Jimenez-Guri, E., Paps, J., Garcia-Fernandez, J. and Salo, E. (2006). Hox and ParaHox genes in Nemertodermatida, a basal bilaterian clade. *Int. J. Dev. Biol.* **50**, 675-679.

Jonsson, J., Carlsson, L., Edlund, T. and Edlund, H. (1994). Insulin-promoter-factor 1 is required for pancreas development in mice. *Nature* **371**, 606-609.

Kojima, H., Nakamura, T., Fujita, Y., Kishi, A., Fujimiya, M., Yamada, S., Kudo, M., Nishio, Y., Maegawa, H., Haneda, M. et al. (2002). Combined expression of pancreatic duodenal homeobox 1 and islet factor 1 induces immature enterocytes to produce insulin. *Diabetes* **51**, 1398-1408.

Kulakova, M. A., Cook, C. E. and Andreeva, T. F. (2008). ParaHox gene expression in larval and postlarval development of the polychaete *Nereis virens* (Annelida, Lophotrochozoa). *BMC Dev. Biol.* **8**, 61.

Lee, P. Y. and Davidson, E. H. (2004). Expression of *Spgatae*, the *Strongylocentrotus purpuratus* ortholog of vertebrate GATA4/5/6 factors. *Gene Expr. Patterns* **5**, 161-165.

Liberzon, A., Ridner, G. and Walker, M. D. (2004). Role of intrinsic DNA binding specificity in defining target genes of the mammalian transcription factor *PDX1*. *Nucleic Acids Res.* **32**, 54-64.

Livi, C. B. and Davidson, E. H. (2006). Expression and function of *blimp1/krox*, an alternatively transcribed regulatory gene of the sea urchin endomesoderm network. *Dev. Biol.* **293**, 513-525.

Livingston, B. T. and Wilt, F. H. (1989). Lithium evokes expression of vegetal-specific molecules in the animal blastomeres of sea urchin embryos. *Proc. Natl. Acad. Sci. USA* **86**, 3669-3673.

Maconochie, M. K., Nonchev, S., Studer, M., Chan, S. K., Pöpperl, H., Sham, M. H., Mann, R. S. and Krumlauf, R. (1997). Cross-regulation in the mouse HoxB complex: the expression of *Hoxb2* in rhombomere 4 is regulated by *Hoxb1*. *Genes Dev.* **11**, 1885-1895.

Martin, E. L., Consales, C., Davidson, E. H. and Arnone, M. I. (2001). Evidence for a mesodermal embryonic regulator of the sea urchin *Cylla* gene. *Dev. Biol.* **236**, 46-63.

Minokawa, T., Rast, J. P., Arenas-Mena, C., Franco, C. B. and Davidson, E. H. (2004). Expression patterns of four different regulatory genes that function during sea urchin development. *Gene Expr. Patterns* **4**, 449-456.

Mlodzik, M., Fjose, A. and Gehring, W. J. (1985). Isolation of *caudal*, a *Drosophila* homeo box-containing gene with maternal expression, whose transcripts form a concentration gradient at the pre-blastoderm stage. *EMBO J.* **4**, 2961-2969.

Nemer, M., Rondinelli, E., Infante, D. and Infante, A. A. (1991). Polyubiquitin RNA characteristics and conditional induction in sea urchin embryos. *Dev. Biol.* **145**, 255-265.

Offield, M. F., Jetton, T. L., Labosky, P. A., Ray, M., Stein, R. W., Magnuson, M. A., Hogan, B. L. and Wright, C. V. (1996). *PDX-1* is required for pancreatic outgrowth and differentiation of the rostral duodenum. *Development* **122**, 983-995.

Oliveri, P., Davidson, E. H. and McClay, D. R. (2003). Activation of *pmar1* controls specification of micromeres in the sea urchin embryo. *Dev. Biol.* **258**, 32-43.

Oliveri, P., Walton, K. D., Davidson, E. H. and McClay, D. R. (2006). Repression of mesodermal fate by *foxa*, a key endoderm regulator of the sea urchin embryo. *Development* **133**, 4173-4181.

Parrington, J., Davis, L. C., Galione, A. and Wessel, G. (2007). Flipping the switch: how a sperm activates the egg at fertilization. *Dev. Dyn.* **236**, 2027-2038.

Ransick, A. and Davidson, E. H. (2006). cis-regulatory processing of Notch signaling input to the sea urchin glial cells missing gene during mesoderm specification. *Dev. Biol.* **297**, 587-602.

Ransick, A., Ernst, S., Britten, R. J. and Davidson, E. H. (1993). Whole mount in situ hybridization shows Endo 16 to be a marker for the vegetal plate territory in sea urchin embryos. *Mech. Dev.* **42**, 117-124.

Rast, J. P., Amore, G., Calestani, C., Livi, C. B., Ransick, A. and Davidson, E. H. (2000). Recovery of developmentally defined gene sets from high-density cDNA macroarrays. *Dev. Biol.* **228**, 270-286.

Rast, J. P., Cameron, R. A., Poustka, A. J. and Davidson, E. H. (2002). *brachyury* target genes in the early sea urchin embryo isolated by differential macroarray screening. *Dev. Biol.* **246**, 191-208.

Sea Urchin Sequencing Consortium: Sodergren, E., Weinstock, G. M., Davidson, E. H., Cameron, R. A., Gibbs, R. A., Angerer, R. C., Angerer, L. M., Arnone, M. I., Burgess, D. R. et al. (2006). The genome of the sea urchin *Strongylocentrotus purpuratus*. *Science* **314**, 941-952.

Smith, M. M., Cruz Smith, L., Cameron, R. A. and Urry, L. A. (2008). The larval stages of the sea urchin, *Strongylocentrotus purpuratus*. *J. Morphol.* **269**, 713-733.

Soltysik-Espanola, M., Klinzing, D. C., Pfarr, K., Burke, R. D. and Ernst, S. G. (1994). Endo16, a large multidomain protein found on the surface and ECM of endodermal cells during sea urchin gastrulation, binds calcium. *Dev. Biol.* **165**, 73-85.

Stoffers, D. A., Heller, R. S., Miller, C. P. and Habener, J. F. (1999). Developmental expression of the homeodomain protein *IDX-1* in mice transgenic for an IDX-1 promoter/lacZ transcriptional reporter. *Endocrinology* **140**, 5374-5381.

Wang, Z., Fang, R., Olds, L. C. and Sibley, E. (2004). Transcriptional regulation of the lactase-phlorizin hydrolase promoter by *PDX-1*. *Am J. Physiol. Gastrointest. Liver Physiol.* **287**, G555-G561.

Weiss, J. B., Von Ohlen, T., Mellerick, D. M., Dressler, G., Doe, C. Q. and Scott, M. P. (1998). Dorsoventral patterning in the *Drosophila* central nervous system: the intermediate neuroblasts defective homeobox gene specifies intermediate column identity. *Genes Dev.* **12**, 3591-3602.

Wessel, G. M. and McClay, D. R. (1985). Sequential expression of germ-layer specific molecules in the sea urchin embryo. *Dev. Biol.* **111**, 451-463.

Wikramanayake, A. H., Peterson, R., Chen, J., Huang, L., Bince, J. M., McClay, D. R. and Klein, W. H. (2004). Nuclear beta-catenin-dependent Wnt8 signaling in vegetal cells of the early sea urchin embryo regulates gastrulation and differentiation of endoderm and mesodermal cell lineages. *Genesis* **39**, 194-205.

Wright, C. V., Schnegelsberg, P. and De Robertis, E. M. (1989). *XlHbox* **8**, a novel *Xenopus* homeo protein restricted to a narrow band of endoderm. *Development* **105**, 787-794.

Wu, L. H. and Lengyel, J. A. (1998). Role of caudal in hindgut specification and gastrulation suggests homology between *Drosophila* amnioproctodeal invagination and vertebrate blastopore. *Development* **125**, 2433-2442.

Yuh, C. H., Ransick, A., Martinez, P., Britten, R. J. and Davidson, E. H. (1994). Complexity and organization of DNA-protein interactions in the 5′-regulatory region of an endoderm-specific marker gene in the sea urchin embryo. *Mech. Dev.* **47**, 165-186.

Yuh, C. H., Bolouri, H. and Davidson, E. H. (1998). Genomic cis-regulatory logic: experimental and computational analysis of a sea urchin gene. *Science* **279**, 1896-1902.

Yuh, C. H., Dorman, E. R. and Davidson, E. H. (2005). *Brn1/2/4*, the predicted midgut regulator of the endo16 gene of the sea urchin embryo. *Dev Biol.* **281**, 286-298.